AGU PUBLICATIONS

JGR

Journal of Geophysical Research: Solid Earth

RESEARCH ARTICLE

10.1002/2016JB012892

Key Points:
- A review of available rock salt creep laws is presented as there is no consensus on flow laws in the literature
- Finite element results for rock salt-capped reservoirs are used to discuss mechanisms by which creep leads to time-varying subsidence
- Results from finite element simulations that test the effects of changing the rock salt flow constitutive model on subsidence are presented

Supporting Information:
- Supporting Information S1

Correspondence to:
G. Marketos,
g.marketos.99@cantab.net

Citation:
Marketos, G., C. J. Spiers, and R. Govers (2016), Impact of rock salt creep law choice on subsidence calculations for hydrocarbon reservoirs overlain by evaporite caprocks, *J. Geophys. Res. Solid Earth*, *121*, 4249–4267, doi:10.1002/2016JB012892.

Received 5 FEB 2016
Accepted 8 JUN 2016
Accepted article online 13 JUN 2016
Published online 29 JUN 2016

Impact of rock salt creep law choice on subsidence calculations for hydrocarbon reservoirs overlain by evaporite caprocks

G. Marketos[1], C. J. Spiers[1], and R. Govers[1]

[1]Department of Earth Sciences, Faculty of Geosciences, Utrecht University, Utrecht, Netherlands

Abstract Accurate forward modeling of surface subsidence above producing hydrocarbons reservoirs requires an understanding of the mechanisms determining how ground deformation and subsidence evolve. Here we focus entirely on rock salt, which overlies a large number of reservoirs worldwide, and specifically on the role of creep of rock salt caprocks in response to production-induced differential stresses. We start by discussing available rock salt creep flow laws. We then present the subsidence evolution above an axisymmetric finite element representation of a generic reservoir that extends over a few kilometers and explore the effects of rock salt flow law choice on the subsidence response. We find that if rock salt creep is linear, as appropriate for steady state flow by pressure solution, the subsidence response to any pressure reduction history contains two distinct components, one that leads to the subsidence bowl becoming narrower and deeper and one that leads to subsidence rebound and becomes dominant at later stages. This subsidence rebound becomes inhibited if rock salt deforms purely through steady state power law creep at low stresses. We also show that an approximate representation of transient creep leads to relatively small differences in subsidence predictions. Most importantly, the results confirm that rock salt flow must be modeled accurately if good subsidence predictions are required. However, in practice, large uncertainties exist in the creep behavior of rock salt, especially at low stresses. These are a consequence of the spatial variability of rock salt physical properties, which is practically impossible to constrain. A conclusion therefore is that modelers can only resort to calculating bounds for the subsidence evolution above producing rock salt-capped reservoirs.

1. Introduction

Extraction of natural gas from a reservoir rock formation leads to pore pressure decrease and so an effective stress increase in the reservoir rock. This in turn causes reservoir compaction and ground deformation which, if of sufficient magnitude, is registered at the surface as subsidence [e.g., *Nagel*, 2001; *Ketelaar*, 2009; *Vasco et al.,* 2008; *Gambolati et al.,* 2006]. Natural gas can be extracted from a variety of reservoir rock types. Here we focus on reservoirs that are capped by rock salt, an impermeable layer that traps the hydrocarbons. Our choice is based on the fact that this reservoir-caprock combination is common worldwide. Examples include the majority of on-shore gas fields in the Netherlands, the key hydrocarbon fields of Brazil [e.g., *Mohriak et al.,* 2012], most of the large fields in the Gulf of Mexico [e.g., *Dribus et al.,* 2008], and the hydrocarbon fields of northwest China [*Yu et al.,* 2014], to name but a few.

In low-lying areas subsidence related to hydrocarbons production can have very important consequences and so needs to be accurately predicted and controlled. Accurate predictions cannot be made, however, if the mechanisms by which subsidence evolves are not fully known [see, e.g., *Hettema et al.,* 2002]. This work focuses on one such mechanism (creep of the rock salt caprock material) highlighting the effects it can have on observed subsidence patterns above a producing gas reservoir. Our previous work [*Marketos et al.,* 2015a, 2015b] has shown that creep of rock salt caprock, in response to shear stresses induced in it by the production process, can, in its own right, produce significant time-dependent ground deformations that will alter the subsidence patterns and their evolution compared with fully elastic analyses. We showed that, if salt creeps according to a linear viscous flow law, the subsidence bowl initially deepens and narrows and then, over large timescales, becomes shallower and wider. In that work, we focused on geomechanical models that were the simplest possible, investigating the system response to a step decrease in pore pressure as applied to the simplest possible reservoir shapes, i.e., shapes approaching point sources (a flat cylinder in 2-D plane strain conditions and a sphere in 2-D axisymmetric conditions—[*Marketos et al.,* 2015a, 2015b], respectively). We

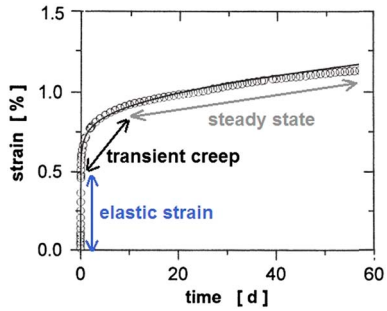

Figure 1. A typical strain versus time plot for a constant stress creep experiment on rock salt at 23°C. Modified from a figure that also appears in *Hunsche and Hampel* [1999].

neglected, among other factors, the effect of depletion rate (i.e., reservoir pressure decrease rate) on subsidence evolution. We treated rock salt as a linear viscoelastic Maxwell material, which is a significant simplification that might only be applicable for fine-grained rock salt undergoing processes such as pressure solution creep at relatively low stresses [*Spiers et al.,* 1990].

In the present paper we investigate a more realistic geomechanical model of a gas reservoir that includes many aspects of the reservoir and subsurface geometry that were absent in our previous work (e.g., layering of material properties, a more realistic reservoir shape, and a full reservoir pressure depletion history associated with production). For example, the pressure depletion history, which was intentionally omitted before, introduces another timescale into the problem, while the use here of nonlinear flow laws makes the response not only time dependent but also dependent on stress levels or flow rates within the rock salt formation. Note though that the reservoir used here is still highly idealized; faults, material layer thickness variations and other complexities are not included for fear of obscuring or masking the effects of rock salt creep. A key, new component of the present paper, compared with our previous work, is a critical analysis of some of the most widely used constitutive models for rock salt flow, noting that (a) there are few direct data to confirm extrapolation of these flow laws to relevant (very low) stresses and strain rates and (b) large uncertainties exist in the literature regarding the rheological processes and parameters that are applicable. The evolution of subsidence as affected by the choice of rock salt creep constitutive model is then explored, examining the effects of some of the flow laws in the context of subsidence evolution above hydrocarbon reservoirs for the first time in the literature. Our geomechanical modeling results and discussion reveal significant effects of creep law choice, i.e., of uncertainties in appropriate rock salt creep law. Our findings for the medium-sized gas reservoir considered are intended to aid practicing engineers to develop insight and methodologies to incorporate these uncertainties into their predictions for subsidence above rock salt-capped hydrocarbon reservoirs around the world.

2. The Creep Behavior of Rock Salt

Figure 1 shows a typical strain versus time plot derived from an axially symmetric compression test on a rock salt sample to which a constant deviatoric (shear) stress is applied at time equals zero. Immediately upon the application of the deviatoric stress, some elastic deviatoric (shear) strain develops (through shortening in the axial direction). Subsequently, the sample undergoes an amount of permanent shear deformation through axial shortening, during a transient period in which the strain rate decreases with time. This eventually gives way to (near) steady state creep, in which the sample deforms at (near) constant strain rate and exhibits behavior that can be described using the concept of viscosity, i.e., the ratio of the relevant measures of shear stress to shear strain rate. Note that the viscosity is in general stress dependent. During both transient creep and steady state creep, the strain rate, as expected, increases with increasing deviatoric stress.

Other boundary conditions for laboratory tests include constant strain rate tests, in which the stress-strain behavior that ensues is generally dependent on the value of the applied strain rate, and stress relaxation tests in which a sample is allowed to deform at fixed load point position following the application of an initial strain and corresponding deviatoric stress. In the latter case, the sample flows so as to relax the shear stresses inside it by converting elastic strain into creep strain, so that the shear stress within the sample decreases to low magnitudes that drive low strain rates over long timescales. Relaxation tests are therefore very relevant to the reservoir problem that motivates this study, especially after the termination of production.

For all of the above types of laboratory experiment, and provided that confining stress is high enough to prevent dilatancy (which is the case for the reservoir geomechanics problem that motivates this study) changes in the mean stress applied to a low-porosity rock salt sample result in mainly "elastic" (i.e., immediate) volumetric strains. This means that volumetric creep strains are very small [see, e.g., *Peach et al.,* 2001]

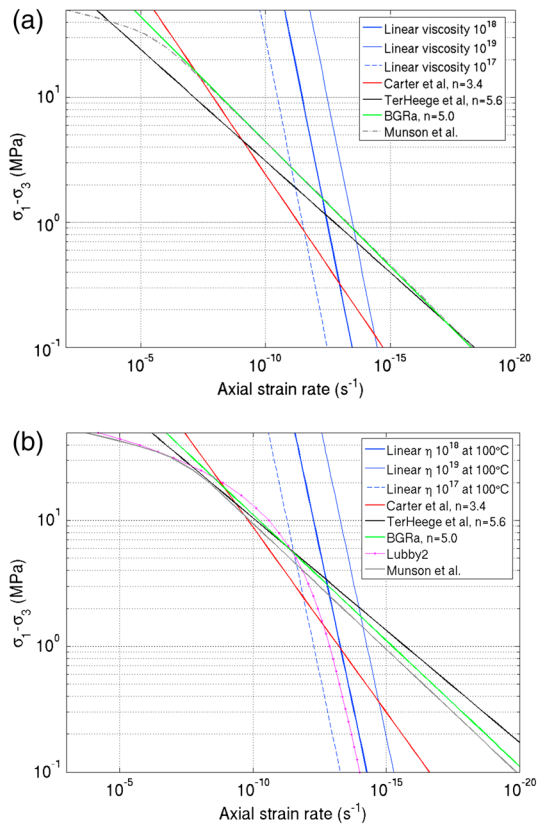

Figure 2. The predictions for principal stress difference in a triaxial compression creep test plotted against axial strain rate for the commonly used flow laws for halite salt that are discussed here. Plots for (a) 100°C and (b) 22°C. Note that not all of the laws will be dominant throughout the whole stress range over which they have been plotted, making some strain rate predictions irrelevant. Note also that the *x* axis has been reversed.

and typically neglected, unless of course microcracks that have not healed already are present in the rock salt sample to start with (such as in, e.g., *Hunsche and Hampel* [1999]). Initially, the discussion here will be focused on steady state rock salt creep; transient creep and its effects will be discussed in a subsequent section.

Constitutive equations or "laws" that describe the steady state creep of rock salt have been traditionally obtained as best fits to data sets derived from laboratory tests similar to the ones described above [e.g., *Carter et al.,* 1993; *Munson and Dawson*, 1979; *Hunsche and Hampel*, 1999]. Laboratory data on the low stress (hence low strain rate) steady state creep behavior of rock salt, however, are scarce as they are very difficult to obtain. They require well-controlled tests that last for months or years and should be conducted under controlled confining pressure, temperature, and humidity conditions that are relevant to the in situ conditions of interest, either directly or via extrapolation (as described, e.g., by *Bérest et al.* [2012]). To achieve practical test durations, a frequently-employed solution has been to extrapolate low stress behavior from higher stress or higher temperature tests, i.e., to use the same rock salt constitutive law for both high and low deviatoric stresses and strain rates. However, extrapolation can be dangerous. This is because a wide range of constitutive laws exist which predict similar viscosities at stresses of 1–10 MPa [e.g., *Carter et al.,* 1993; *Munson and Dawson*, 1979; *Hunsche and Hampel*, 1999; *Spiers et al.,* 1990; *ter Heege et al.,* 2005a] but whose viscosity prediction at low stress varies by several orders of magnitude (see, e.g., Figure 2). Nonetheless, in many cases, including the reservoir geomechanics application that motivates this study, the low deviatoric stress creep of rock salt is critically relevant. Indeed, the choice of an appropriate low-stress rock salt flow law is of major importance as extrapolation of the different flow laws available can have important effects on the calculation results. In order to decrease uncertainties and to make as educated as possible a choice of rock salt creep constitutive model, the only possible solution is linkage of the observed macroscopic response to the grain-scale process responsible for deformation. This issue will now be considered.

The microscale processes that lead to creep of rock salt can be broadly separated into three categories (see review by *Urai et al.* [2008]): ones that involve motion of dislocations inside the crystal lattice of the individual grains composing the rock salt (dislocation creep), ones that involve water-assisted diffusive transport of material down normal stress gradients set up around the boundaries of individual salt grains (pressure solution or solution precipitation creep) and ones that involve dilatancy and damage to the rock salt as a result of brittle and plasticity-coupled microcrack growth (brittle creep). The current discussion will focus on the first two grain-scale processes, as they are the ones relevant to the reservoir geomechanics application which motivates this study, where the mean stress is high enough in comparison to the shear stress so that dilatant behavior and the opening of cracks inside the rock salt is suppressed (see, e.g., *Hunsche and Hampel* [1999] or *Horii and Nemat-Nasser* [1985] for a description of the process). Dilatant behavior is of course possible and important in relation to other problems, such as cavern integrity modeling in salt mines or the stability of wells drilled through salt.

Provided that traces of water are present in thin, connected grain boundary films or microchannel networks, which is believed to be the case in natural salt at least when deviatoric stresses are not too low [see *Urai et al.,* 2008; *Desbois et al.,* 2010], both dislocation creep and pressure solution creep can occur simultaneously. It is generally assumed that such processes are independent of each other and act in parallel, so that steady state strain rates calculated for them can be added to obtain the total steady state strain rate for rock salt [see, e.g., *Spiers and Carter,* 1998; *Urai et al.,* 2008]:

$$\dot{\varepsilon}_{\text{total}} = \dot{\varepsilon}_{\text{disloc}} + \dot{\varepsilon}_{\text{pres.sol}} \tag{1}$$

It is widely accepted that each of the steady state strain rate terms here can be expressed through an equation of the following form:

$$\dot{\varepsilon} = A \cdot e^{-Q/RT} \cdot \sigma^n \tag{2}$$

where A is a constant that is inversely dependent on the cube of grain size for pressure solution in salt, Q is an activation energy (expressed in J/mol), R is the universal gas constant (8.314 J/mol/K), T is the temperature in Kelvin, n is a unitless stress exponent, and σ the shear stress [e.g., *Spiers et al.,* 1990; *Carter et al.,* 1993; *Hunsche and Hampel*, 1999; *ter Heege et al.,* 2005a]. Note that many published flow laws are expressed as relations between axial strain rate and principal stress difference in a triaxial laboratory experiment (i.e., $\dot{\varepsilon}$ is often the axial strain rate and σ the difference between axial and radial stresses). Equations similar to (1) and (2) are valid and widely applied for numerous crystalline materials that exhibit dislocation creep and diffusion creep [*Frost and Ashby,* 1982]. Note that $n = 1$ means that the creep law is linear, which is the case for pressure solution creep. For dislocation creep processes in materials ranging from metals to ceramics and minerals, including rock salt, n typically falls in the range 3–6. Such behavior is often referred to as power law creep and is insensitive to grain size. By virtue of the different elementary processes involved, dislocation creep and pressure solution in salt of course also display different activation energies Q (a value for which one might be able to independently calculate from theoretical arguments as attempted by *Wawersik and Zeuch* [1986], for example), and a different A value. These differences lead to a different dependence on stress and temperature meaning that the rate-controlling microscale process can change if stress or temperature changes [*Urai et al.,* 2008]. Failure to recognize this can lead to an empirical fit to flow data that works well at the conditions of the corresponding laboratory tests but which fails when extrapolating to different stresses or temperatures [see *Carter et al.,* 1993; *Muhammad et al.,* 2012; *Günther et al.,* 2015]. For salt, the typically observed values of Q and n for pressure solution and dislocation creep in equation (2) imply that pressure solution should dominate at low stresses and temperatures versus dislocation creep at higher stresses and temperatures [*Urai et al.,* 2008]. Here it should be noted that some rock salt creep laws (e.g., the Lubby2 model, described by *Lux and Heusermann* [1983] and incorporated in the more elaborate Lux/Wolters model—see, e.g., *Wolters et al.* [2012] and discussion by *Blanco Martín et al.* [2015]—or one term in the *Munson et al.* [1990] model) express the steady state creep term using a different functional form. These different functional forms attempt to empirically capture the transition from flow rates that are controlled by one grain-scale mechanism to ones controlled by another. This transition happens at differential stresses higher than 20.5 MPa for the *Munson et al.* [1990] and so is not so relevant for the application considered here. For the Lubby2 creep law (see Figure 2) the transition happens at much lower stresses. Lubby2 is therefore able to mathematically capture the transition from the rates being controlled by dislocation (power law) mechanisms to ones controlled by pressure solution creep (linear), if the temperature is constant. However, the fact that this law is empirical does not allow safe extrapolation to temperatures (or stresses) for which it is not calibrated or validated.

From microstructural studies of rock salt deformed under natural geological conditions [see *Urai et al.,* 1987, 2008; *Schléder and Urai*, 2007; *Schléder et al.,* 2007; *Desbois et al.,* 2010], there is abundant evidence that deformation at low, natural stresses and strain rates involves dislocation creep, fluid-assisted grain boundary migration (due to transfer of mass across fluid-filled grain boundary films [*Peach et al.,* 2001]) and pressure solution (transfer of mass along fluid-filled grain boundaries [*Spiers et al.,* 1990]), though whether operation is simultaneous as opposed to sequential is not always clear. While these processes have all been observed in various experimental studies referred to above, there is still controversy about the role of water and whether pressure solution is important during natural salt flow at low stresses. Pressure solution is fluid assisted but requires only very small amounts of water to occur (>10–20 ppm, [*Urai and Spiers*, 2007]). Most natural rock

Table 1. The Parameters for the Halite Salt Creep Laws Used Here[a]

	n	A (MPa^{-n} s^{-1})	Q (kJ/mol)
Carter et al. [1993]	3.4 ± 0.1	$8.1 \times 10^{-5} \pm 2.7 \times 10^{-5}$	51.6 ± 1.2
Spiers et al. [1990]	1.0	$(3.76 \times 10^{-13} \pm 1.89 \times 10^{-13})/T/D^3$ effective grain size (D) and temperature (T) dependent	24.5 mean value
ter Heege et al. [2005a]	5.6 ± 0.5	$10^{-1.56 \pm 0.54}$	80 ± 6
Hunsche and Hampel [1999] (BGRa)	5.0 mean value	2.1×10^{-6} mean value	54 mean value

[a]Refer to equation (2) where $\dot{\varepsilon}$ is the axial strain rate and σ the difference between axial and radial stress in a triaxial laboratory test.

salt samples contain enough water, but their generally quite coarse grain size (5–20 mm) means that pressure solution is too slow to be observed on standard lab time scales and is only directly detected in fine, synthetic samples [*Urai et al.,* 1986; *Spiers et al.,* 1990]. Moreover, a large number of the tests in the literature have been performed on samples that may have lost their free water content during storage or during testing itself, especially in the case of unconfined creep tests at elevated temperature. Water loss in this way will inhibit pressure solution leading to results that may be unrepresentative, with the measured sample viscosity potentially being much higher than in situ, especially if the grain size is low.

All of these points have led to the role of pressure solution during natural low stress flow of rock salt being questioned, despite clear evidence for solution precipitation transfer and the existence of intergranular fluid films in naturally deformed samples [e.g., *Urai et al.,* 1986, 1987; *Desbois et al.,* 2010]. A further argument suggesting that pressure solution may not operate at low stresses, and that flow may be ubiquitously dominated by dislocation creep, stems from the theoretical possibility that at sufficiently low-stress intergrain boundary healing could disconnect the grain boundary fluid pathway through which ionic diffusion from high- to low-stress grain contacts occurs and so block pressure solution [*van Noort et al.,* 2008]. This might be to some extent supported by numerical calculations reported by *Li et al.* [2012] that show that dense anhydrite stringers present in naturally deformed rock salt bodies do not sink through the salt, which seem to imply that viscosities are much higher than what were calculated for pressure solution. However, there could be other explanations for the observations of Li et al., notably the presence of sufficient anhydrite inside the rock salt body in question, which could slow down the sinking of these stringers.

In addition to the above uncertainties in the importance of pressure solution during natural salt flow, and to the difference in dislocation creep laws obtained for salts of different composition [see, e.g., *Wawersik and Zeuch,* 1986], the fact that pressure solution strain rate is inversely proportional to the cube of the effective grain diameter [see *Spiers et al.,* 1990] implies high sensitivity to uncertainties in the grain size of natural salt formations. This can have major implications as rock salt with millimeter grain size can flow 3 orders of magnitude faster than with centimeter grain size, still potentially dominating over dislocation creep if stresses are high enough to avoid grain boundary healing.

There is, therefore, no clear consensus at present as to which flow law best describes rock salt behavior at the stress range relevant to this study. Analyses will be therefore presented here that incorporate the most commonly used flow laws so as to investigate the full range of possible geomechanical model responses and to assess to what extent flow law choice can affect subsidence calculations above a producing gas reservoir. In addition to the linear pressure solution flow law due to Spiers and coworkers discussed above [e.g., *Spiers et al.,* 1990], commonly used steady state, power law creep equations for natural rock salts having a stress exponent of 3–5 (*Carter et al.* [1993], *Hunsche and Hampel* [1999], often referred to as BGRa, or *Munson and Dawson* [1979]) and believed to describe dislocation creep, will be explored. We also consider the flow law with stress exponent (n) of 5.6 obtained by *ter Heege et al.* [2005a] for wet salt deforming by dislocation creep coupled with fluid-assisted dynamic recrystallization. This behavior appears to represent a balance between pressure solution and dislocation creep processes that leads to a steady state grain size for a particular shear stress range. Note, however, that this balance requires rather high shear strains to fully develop (>5–10%), so that the ter Heege et al. flow law may not be directly relevant to the present reservoir geomechanics application.

Table 1 lists the parameters for the flow laws discussed and implemented as part of this study for halite rock salt. Figure 2 plots these laws (and two others) in stress-strain rate space at 100°C and at 22°C, the latter only shown so that the reader can appreciate what the temperature dependence of these creep laws is. Note that

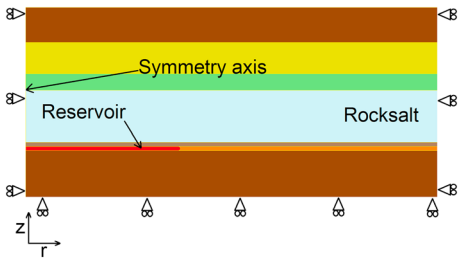

Figure 3. A sketch of the geometry for the simplified finite element analyses presented here (to scale around the model reservoir but bottom and right edge truncated). Note that rollers are applied along the entire side over which they are drawn.

some of the laws might not be dominant throughout the whole stress range over which they have been plotted, while others, though commonly used, might not be the best option for the application discussed here. Also, in many cases rock salt is not pure halite but contains subordinate amounts of other evaporite minerals (see, e.g., *Coelewij et al.* [1978] and *Raith et al.* [2015] for discussion of a special case) which have typically been deposited as part of a sequence of drying up and reflooding events. Often, there is very little information on the mineral composition of a rock salt body, and so this will be treated as an extra complexity, the potentially important consequences of which are beyond the scope of this study.

3. Method

Geomechanical analyses of a simplified representation of a producing gas reservoir have been conducted. The serial version of the in-house Lagrangian Finite Element software package GTECTON is used to solve for stress equilibrium, material strain, and displacements [*Govers and Wortel,* 1993, 1995]. In GTECTON, the resultant matrix equations are solved using PETSc (see PETSc user manual [*Balay et al.,* 2002]). This is done iteratively [*Govers and Wortel*, 2005], and geometrical nonlinearity is accounted for by application of a residual force update scheme [*Hall-Wallace and Melosh*, 1994; *Govers and Wortel*, 1999]. The analyses conducted here use constant strain triangles with the mesh sufficiently refined around the axis of symmetry and other points where stresses or displacements vary rapidly (e.g., the reservoir, the rock salt, and the boundaries between the rock salt and other layers), so as to ensure an accurate solution. An advantage of using GTECTON for the present work is that we have full access to the source code and so could easily modify it to implement any rock salt flow law necessary. The software itself has been validated for a number of problems against known solutions (e.g., against *Verruijt* [1996] and *Gerya* [2010]) and has been extensively used to solve for stresses and displacements inside the Earth's lithosphere and upper mantle [e.g., *Furlong and Govers*, 1999; *Buiter et al.,* 2001; *Schmalzle et al.,* 2006; *de Franco et al.,* 2007; *Riva and Govers*, 2009; *Baes et al.,* 2011; *Plattner et al.,* 2013]. As a reservoir that exhibits cylindrical symmetry is analyzed here, the axisymmetric version of the code is used. Hence, stresses, strains, and displacements are only calculated on a 2-D vertical cross section that passes through the center of the reservoir (see Figure 3). The full 3-D problem can be reconstructed by revolving this cross section through 360°.

All materials are assumed isotropic and elastic, apart from the rock salt, which is assumed to be isotropic viscoelastic. The constitutive equations used are (for axisymmetric conditions)

$$\dot{\varepsilon}_{rr} = \frac{1}{E}\left(\dot{\sigma}_{rr} - \nu\left(\dot{\sigma}_{zz} + \dot{\sigma}_{\theta\theta}\right)\right) + \frac{2\sigma_{rr} - \sigma_{zz} - \sigma_{\theta\theta}}{6\eta} \tag{3}$$

$$\dot{\varepsilon}_{rz} = \frac{1+\nu}{E}\dot{\sigma}_{rz} + \frac{\sigma_{rz}}{2\eta}, \dot{\varepsilon}_{r\theta} = 0, \dot{\varepsilon}_{\theta z} = 0 \tag{4}$$

where E, ν, and η are the material Young's modulus, Poisson ratio, and the shear viscosity, respectively. For nonlinear creep laws η signifies the viscosity at the particular element stress. Parameters σ and ε are the stress and strain with a dot over the symbol signifying the rate of change with time, and subscripts r, z, and θ denoting the radial, vertical, and tangential (i.e., horizontal into the page) directions, respectively. A similar equation to equation (3) applies to the strain rates in the other directions ($\dot{\varepsilon}_{zz}$ and $\dot{\varepsilon}_{\theta\theta}$) and $\dot{\varepsilon}_{r\theta}$ and $\dot{\varepsilon}_{\theta z}$ are zero due to symmetry. Note that the above equations revert to the ones for an elastic material for infinite material viscosity. Also note that the equation for $\dot{\varepsilon}_{zz}$ can be used to obtain the shear viscosity to be used as input to the simulations for flow laws published in the literature which are often presented in the form of as axial strain rate versus principal stress difference ($\sigma_{zz} - \sigma_{rr}$) in a triaxial laboratory test.

In the above equations stresses are on top of gravity-induced stresses. Gravity-induced stresses can be safely neglected provided that at the start of the time-dependent deformation, the domain is in static equilibrium. It

Table 2. Material Properties and Depths of the Rock Units Used in the Simulations Reported Here

Unit Name	Young's Modulus (GPa)	Poisson Ratio	Depth Range for the Unit (m)
North Sea	2	0.30	0–850
Chalk	10	0.25	850–1600
Lower Cretaceous/Triassic	16	0.25	1600–2000
Rock salt (Zechstein)	30—but viscoelastic	0.35	2000–3250
Ten Boer	40	0.20	3250–3350
Rotliegendes (reservoir)	20	0.20	3350–3450
Carboniferous	40	0.20	3450–39600

is only perturbations from the equilibrium configuration that cause ground displacements, and shear stresses inside the rock salt are assumed to be zero initially (i.e., fully relaxed). If there are unrelaxed shear stresses within the rock salt at the start of production, the potential exists for locally slightly higher shear stresses than the ones appearing in the results presented. These will only have an effect on rock salt strain rates for power law rheologies. Unrelaxed stresses might need to be included in the geomechanical model for tectonically active regions where rock salt is actively deforming prior to production, but they are thought to be unimportant for tectonically inactive regions such as the Netherlands, whose gas fields motivate this study. Note also that unrelaxed stresses might exist in natural rock salt if rock salt creep does not continue all the way to zero shear stresses (see discussion in section 8.3). Density differences between the salt and surrounding layers are neglected in our models; it is argued that the strength of the surrounding layers is sufficient to inhibit salt diapirism, and even if it occurred it would develop over the timescales much larger than the ones relevant to the gas extraction problem.

Gas production induces a pore pressure decrease inside the porous reservoir rock. Assuming that the reservoir is effectively sealed from its surroundings by the impermeable rock salt cap and impermeable faults at its edges, any such pore pressure decrease will be fully maintained after production. Here consistent with the theory of poroelasticity and Terzaghi's effective stress principle [see, e.g., *Bolton*, 1991], we model the reservoir pore pressure decrease as an externally applied mean compressive (effective) stress increase that is applied uniformly throughout the isotropic and elastic porous material within the reservoir. The motivation behind applying this mean stress increase is that it is the effective stress, i.e., the total stress minus the pore fluid pressure (if the sign convention in compression is positive) that is assumed to be carried by the solid material skeleton of the porous material, and so, linked to the material strains through the reservoir elastic moduli (equation (3)). Here by assuming a reservoir system that is fully sealed from its surroundings, any reservoir pore pressure decrease due to production will directly lead to an increase in mean effective stress in the reservoir, in proportion to the reservoir pore pressure decrease (or equal to it if the poroelasticity coefficient is 1). Assuming a high enough permeability reservoir layer, pore pressures will immediately equilibrate inside it, and so the same mean stress increase can be applied throughout the whole reservoir. Note that poroelasticity effects can be safely neglected for the very low porosity rock salt layer. Here we also neglect the poroelastic response of the other layers. These will be anyway small away from the reservoir but can be significant for the often poorly sampled rock underlying the reservoir or if the lateral boundaries of the reservoir are permeable.

4. The Geomechanical Model for a Rock Salt-Capped Reservoir

The reservoir model used here is a somewhat idealized representation of a typical Dutch gas field (see Figure 3 for a sketch of the model). The layering and material properties typical of the north of the Netherlands subsurface have been used (see Table 2 after *Nederlandse Aardolie Maatschappij (NAM)* [2013], for example). Note that, usually, a range of reservoir material elastic moduli are quoted, as the value is site specific, while sublayering inside the reservoir is also often included in detailed models. Here we use a midvalue of 20 GPa. It should also be noted that the exact modulus value controls the volume strain at the reservoir due to the pore pressure decrease and so severely affects the magnitudes of surface subsidence but has been observed to have only very minor effects on subsequent normalized subsidence trends. Modulus degradation due to possible reservoir rock inelasticity or creep is neglected. In the analyses layers are set to be horizontal and extend to the edges of the domain for the simulation, itself placed at a distance of 56 km from the reservoir center. This includes the Rotliegendes sandstone formation, only part of which is

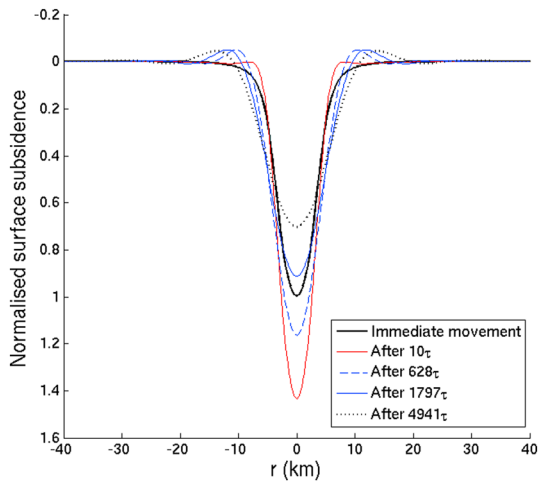

Figure 4. The subsidence bowl plotted at a number of different times after the step application of the reservoir pore pressure decrease. Displacements are normalized by the maximum subsidence value at $t = 0$ and time by the Maxwell time (τ) for the linear viscoelastic rock salt material.

the reservoir. Note further that all materials are assumed isotropic and elastic, apart from the rock salt (Zechstein) layer which is modeled as an isotropic viscoelastic Maxwell material (see equation (3)). Tilts in the geological layers and nonhomogeneities within layers have been neglected as the first-order sensitivity of the model to the rock salt creep law is sought here. The effect on subsidence trends of changes in the material properties of different layers not immediately adjacent to the reservoir will be small and so is ignored in this study. This study instead focuses on the much larger effects of the choice of rock salt creep law on the calculated subsidence evolution for the specific geomechanical model considered.

The reservoir itself is centered at a depth of 3400 m and is a disk of radius 3.75 km and height 100 m. This reservoir thickness is typical of the Dutch gas reservoirs [see *NAM*, 2010, Table 7.1], and the depth of the reservoir is also typical, while the lateral extent of the reservoir varies significantly for the Dutch gas fields. The radius of curvature of its edges is 50 m, which was done to maintain consistency with previous models described by *Marketos et al.* [2015a, 2015b]. This radius of curvature will not affect subsidence results significantly. The effect of the reservoir lateral extent will be touched upon with subsequent work, but preliminary simulations suggest that it is very important for the magnitude of time-varying subsidence. *Marketos et al.* [2015a] discuss the sensitivity of the subsidence response to the thickness of the rock salt layer, which is set here to 1250 m. Initially, the response to a step pore pressure reduction is presented and then the response to a more realistic pore pressure reduction history is shown.

5. The Step Response of the Linear Geomechanical Model

As discussed above it is likely that the bulk of rock salt creep will be through pressure solution, a grain-scale process that leads to a linear flow law. In this case the rock salt viscosity is independent of the stress level but grain size dependent and proportional to the third power of grain size. The grain size of salt is typically unknown as it is costly to obtain rock salt samples from the cap rock due to associated drilling challenges. *Breunese et al.* [2003] quote average grain sizes of between 3 mm and 20 mm for rock salt from a rock salt layer in the north of the Netherlands. This variation itself leads to over 2 orders of magnitude variations in viscosity, highlighting the associated uncertainties. Nevertheless, the step response of linear models with different viscosity can be unified by normalizing time by the salt Maxwell time (τ, the ratio of its shear viscosity to its shear modulus). Essentially, the Maxwell time is a descriptor of how fast flow occurs inside the material and so provides a timescale for material response. It represents the decay time constant in the exponential that describes the evolution of shear stresses in a Maxwell material element to which a step increase of shear strain is applied, i.e., the time at which the rock salt element's shear stress has reached $1/e$ (i.e., 36.8%) of its value just after the strain application.

The use of the linear rock salt flow law is also a starting point for rationalizing the subsidence response, as in that case superposition of solutions can be used to build the response to a complex time-dependent input. For example, for a linear geomechanical model, the subsidence will be proportional to the pore pressure reduction at the reservoir level. Also, the response to a pore pressure depletion history can be built up as the convolution of the step response of the system with the input pore pressure decrease. Hence, understanding the step response of the system, i.e., the subsidence evolution after the application of a constant pore pressure reduction at the reservoir level becomes very important. The step response has been discussed previously by *Marketos et al.* [2015a] for a simplified cylindrical reservoir under 2-D plane strain conditions and by *Marketos et al.* [2015b] for an axisymmetric spherical reservoir in geomechanical models with no

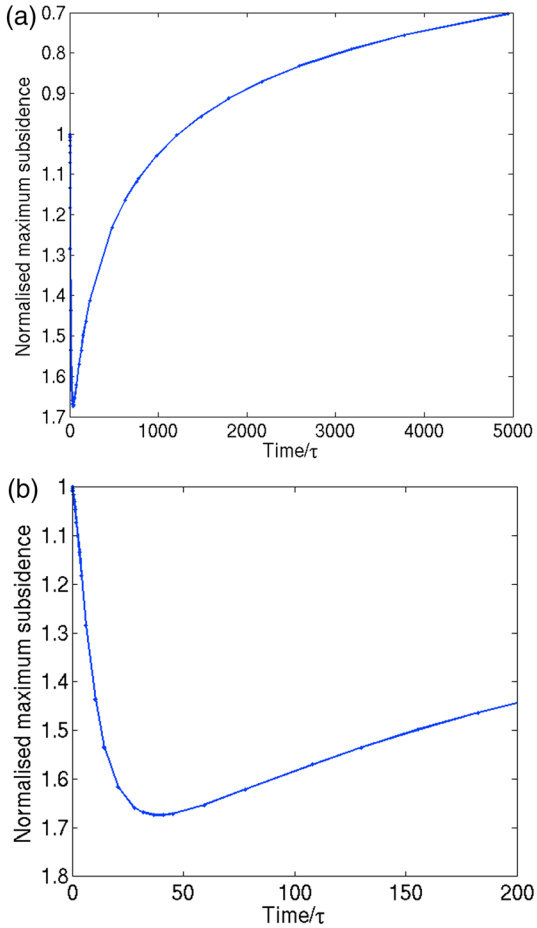

Figure 5. The evolution of maximum surface subsidence (i.e., at point $r = 0$, $z = 0$) after the step application of the reservoir pore pressure decrease. Displacements are normalized by the maximum subsidence value at $t = 0$ and time by the Maxwell time (τ) for the viscoelastic rock salt material. (a) the curve up to 5000 Maxwell times (b) a zoomed-in version of the same plot.

material layering. As the behavior for the more complex reservoir studied here is very similar, this will only be briefly described here.

Figure 4 plots a cross section of the subsidence bowl at its middle for a number of time instants after the reservoir pore pressure decrease, which is applied here instantaneously. The immediate response to the application of the step pore pressure reduction is that of compaction of the reservoir, which appears immediately at the ground surface as subsidence (the elastic response, see Figure 4, solid black curve). Initially, the subsidence bowl becomes deeper and narrower. At later stages, the subsidence bowl becomes shallower and wider. Note that to reconstruct the 3-D shape of the bowl, the curves below have to be revolved by 180° about the point $r = 0$. This means that even though it seems that the volume lost at the surface (i.e., the volume between the plane at $z = 0$ and the subsidence bowl surface) changes significantly with time, this is not the case. The initial deepening of the subsidence bowl at r close to zero is balanced out by the fact that the bowl becomes narrower, and so there is an upward movement at the surface for regions at a larger radial distance, i.e., over larger areas.

Even though not shown here, we have checked that the volume lost at the surface is almost exactly equal to the volume lost at the reservoir level (i.e., reservoir volumetric strain) and that salt flow and subsidence redistribution has little effect on the total volume lost at the surface. Note, however, that there will be parts of the area above a gas field that see local volume loss and others that see local volume increase. Any increases or redistribution of volume lost due to the gas extraction are very relevant for the sediment budget in sensitive coastal areas and so need to be considered when the environmental imprint of the pumping is assessed [*van Thienen-Visser et al.,* 2015]. Finally, though not shown here, there are significant horizontal displacements too, as shown by *Marketos et al.* [2015a], for a simpler geomechanical model. Horizontal displacements amount to approximately half of the elastic surface subsidence and so could contain invaluable information as to the subsurface macroscale mechanisms through which subsidence develops. It is therefore wise to measure these in the field wherever possible.

Figure 5 shows the evolution of subsidence for the point at $r = 0$, i.e., the deepest point of the subsidence bowl for the same simulation. Tracking the vertical displacement of this point is useful as it provides a scalar measure for quantifying the changes shown in Figure 4. Maximum subsidence is also an important quantity in subsidence calculations, as it sometimes needs to be limited below a certain value as part of a gas extraction contract. As can be seen, the observations of Figure 4 are echoed in Figure 5. There is an initial relatively fast deepening of the subsidence bowl followed by a much slower rebound. These two distinct types of behavior can be associated with two distinct displacement mechanisms, as discussed by *Marketos et al.* [2015a]. Initially, it is the relatively rapid relaxation of rock salt shear stresses driving the deformation, which is responsible for the increase in maximum subsidence. This we term *the shear stress flow mechanism*. At later stages a

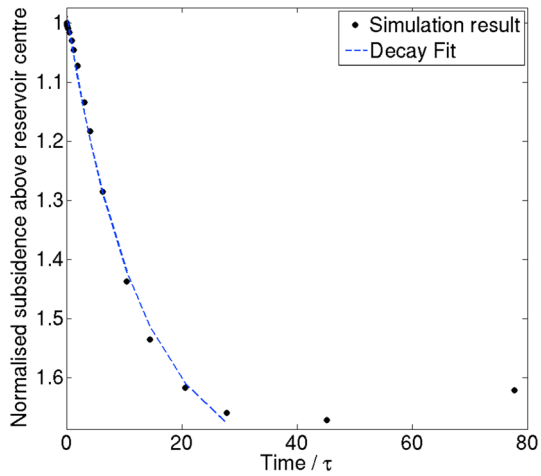

Figure 6. A zoomed-in version of Figure 5 that includes an exponential decay best fit line to the simulation results.

pressure flow mechanism becomes dominant, which leads to a rebound of maximum subsidence. In this second mechanism the rock salt behaves more like a fluid, and deformation is through flow within the confined conduit of the rock salt layer. This flow is driven by small mean stress (rock salt pressure) differences within the salt layer which are eventually dissipated. For the geomechanical model presented here the change of shape of the subsidence bowl for times larger than 50 τ (i.e., for when pressure flow is dominant) can be explained through rock salt volume redistribution; there is thickening of the rock salt layer above the centerline of the reservoir that is approximately equal to the amount of subsidence rebound developed.

Marketos et al. [2015a] discuss the effect of the thickness of the rock salt layer on the relative strength of these two mechanisms, which has a strong effect on the maximum subsidence versus time curve. Essentially, the thicker the rock salt above a gas reservoir the faster the pressure flow mechanism. This means that the maximum subsidence is attained earlier in time, and the maximum subsidence is reduced for thicker rock salt layers. Finally, note that, as will be discussed later, the pressure flow (and eventual subsidence rebound) is not observed in models where rock salt flow is through power law creep only.

6. Time Decay fit of the Initial Maximum Subsidence Step Response Curve

The initial parts of the maximum vertical subsidence versus time plot (Figure 5) follow a curve that can be approximated by an exponential decay function ($e^{-t/\tau_{\mathrm{app}}}$). Such empirical exponential time decay has been suggested as a good fit of the limited field subsidence data available [e.g., *NAM,* 2013; *Mossop*, 2012]. Figure 6 shows the step response of the geomechanical model up to 80 Maxwell times and a least squares exponential decay fit to the data. As with the simpler models [*Marketos et al.,* 2015a], this empirical fit to the initial subsidence data is relatively good. It yields an apparent decay time (τ_{app}) of 12.8 Maxwell times (τ) when all data points below 30 τ are used. Note that the apparent decay time depends on the number of data points used for the fit. Also, the exponential decay fails to capture the response at times larger than approximately 40 τ, where the second mechanism discussed above is active (i.e., "pressure flow" or mean stress equilibration inside the rock salt layer), and significant rebound is predicted by the analysis. Finally, the apparent decay time is proportional to the rock salt Maxwell time (τ) but as discussed by *Marketos et al.* [2015a] the geometry of the problem is seen to be a very important controlling factor on its exact value. For example, geomechanical models with a thinner salt layer would take longer to respond to the pore pressure perturbation at the reservoir and so have a higher apparent decay time.

The implications of describing the initial response with such a simple exponential curve are important. If the geomechanical model is linear, then superposition of solutions can be used to calculate the initial subsidence response to any complex reservoir pore pressure decrease input in a fast and inexpensive way. Note, however, that fitting of the later parts of the subsidence curve would be necessary if the full subsidence response is required; this might be achieved through the use of another simple exponential decay function and a possible time delay, i.e., through the use of three additional parameters. In the case of power law rock salt flow, the system is no longer linear and so superposition of solutions does not hold. However, in this case the exponential decay fit describes the overall behavior much better than in the linear rock salt flow case (as subsidence rebound is not observed, see below). It could be then that an initial geomechanical system decay time might be used as a single scalar quantity to quantify the subsidence response of reservoirs. This could be further used to characterize their relative subsidence redistribution potential, i.e., form the basis of a reservoir classification scheme.

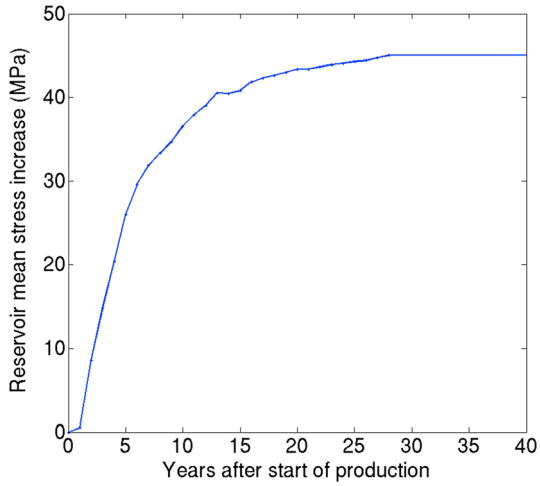

Figure 7. The applied reservoir sandstone mean stress increase versus time. This is used as an input to the axisymmetric geomechanical model in this subsection.

7. The Response to a Full Gas-Pumping History

Typically, the gas field operator monitors pressures at the well. Using some assumptions and sometimes even a reservoir simulator, these point measurements of pressure can be used to estimate the spatial distribution of pore pressure inside the reservoir material. This can be further constrained by the total gas volume produced. As discussed above, here we apply the reservoir pore pressure reduction as a uniform spatially, externally applied mean stress increase throughout the reservoir volume. This is what causes compaction of the reservoir and the rock salt shear stresses that drive further subsidence time dependence. Figure 7 shows the value of the applied mean stress increase in the reservoir region. We assume that after 28 years, gas pumping stops and reservoir pore pressure remains constant.

The maximum subsidence versus time is plotted in Figure 8 for a linear rock salt creep law and viscosity values of 10^{17} Pa s, 10^{18} Pa s, and 10^{19} Pa s. These values correspond to effective grain sizes of 4.8, 10.4, and 22.4 mm, respectively, at a temperature of 100°C if the mean values of the coefficients for the grain size versus viscosity equation given in *Spiers et al.* [1990] are used. Note that these values cover the mean grain size range of between 3 and 20 mm that is reported for a north of the Netherlands Zechstein layer by *Breunese et al.* [2003].

In rationalizing the response of the reservoir to different rock salt viscosities the ratio of the timescales for pressure drawdown to the timescale for system response emerges as an important quantity. Note that for the linear rock salt the timescale for system response is proportional to the salt Maxwell time (as discussed above), but as discussed in *Marketos et al.* [2015a] the system depends strongly on the rock salt layer thickness (among others), i.e., is geometry dependent. More work is needed so as to predict quantitatively this geometrical dependence; at the moment it can only be deduced by conducting sets of finite element simulations.

The simulation for a viscosity of 10^{19} Pa s shows hardly any shear flow-driven subsidence during the first 28 years as can be seen by comparing with the curve for an elastic salt layer (i.e., infinite salt viscosity). The rock salt element response time in this case (Maxwell time) is relatively high at 28.5 years, and the apparent decay time of the system, which is more than 12 times this, is much larger than the gas production period (28 years). Therefore, little subsidence beyond the elastic amount occurs during gas pumping. As is clear from the red curve, subsidence increase occurs subsequently over a millennium period. Both the 10^{17} and 10^{18} Pa s curves show significant shear flow-driven subsidence during the first 28 years, as in these cases the apparent system decay time and the pumping period are comparable. The model with a viscosity of 10^{17} Pa s displays the fastest deviation from the elastic response curve. As here pressure flow and subsidence rebound starts even before pumping is stopped, the maximum subsidence attained is smaller than what is observed for the case of viscosities of 10^{18} and 10^{19} Pa s.

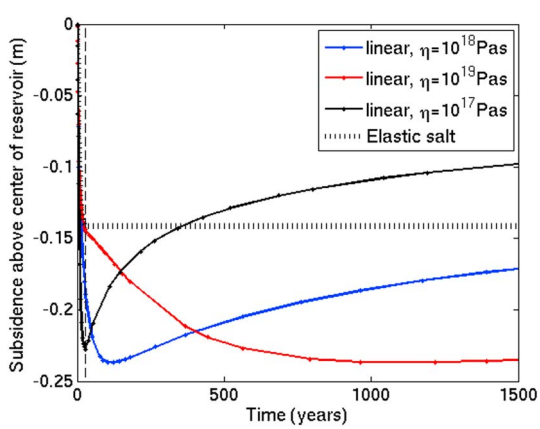

Figure 8. The evolution of maximum subsidence for the model where a realistic reservoir pore pressure history is applied. Results for a number of viscosities and a linear rock salt flow law. The vertical broken line represents end of pumping history, i.e., 28 years.

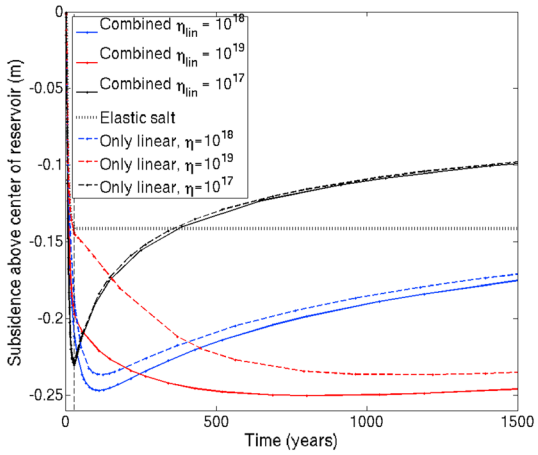

Figure 9. The evolution of maximum subsidence for the model where a realistic reservoir pore pressure history is applied. Results for a combined linear and Carter et al. power law flow (solid lines). Results for the corresponding linear only flow law included for reference (dashed lines). The broken vertical line represents end of pumping history, i.e., 28 years.

This is an important result—it indicates that in the case of linear salt flow it might be possible to constrain the maximum subsidence value to a certain percentage over the subsidence measured at the end of pore pressure depletion. Note, however, that the time the maximum subsidence will be attained is a function of the salt viscosity. The times at which the maximum subsidence is reached are proportional to the rock salt viscosity for rock salt layers with Maxwell times that are large in comparison to the time period through which the forcing is applied while they are affected by the reservoir pressure depletion history in cases where the rock salt Maxwell times are low. A major problem for modelers, however, is that the value of rock salt viscosity is usually poorly constrained as grain size data on salt are typically not available.

8. Response to Different Salt Flow Laws

8.1. Use of a Combined Linear and the *Carter et al.* [1993] Flow Law

For the simulations presented in this subsection a combined linear (pressure solution) and power law creep constitutive model is used, with the power law creep described by the parameters of *Carter et al.* [1993] ($n = 3.4$, see Table 1). Essentially, at low stresses linear creep (i.e., a pressure solution creep) controls the rate, while at higher stresses the power law (i.e., dislocation creep) takes over. Note that pressure solution creep is grain size dependent while dislocation creep is grain size independent. Figure 9 shows the evolution of the maximum subsidence. Adding power law flow to an already low viscosity of 10^{17} Pa s (the value calculated for rock salt with an effective grain size of 4.8 mm at 100°C when using the mean values of the coefficients given in *Spiers et al.* [1990]) has little effect on the observed subsidence; results are the same as for when only linear rock salt creep is active. This is because the point at which the two relevant curves intersect is at a relatively high differential stress (approximately 1 MPa, see Figure 2), and so the flow of the bulk of the rock salt, which is at a relatively low differential stress, will follow a linear law anyway for low viscosity values.

For higher values of the linear viscosity (i.e., for the higher rock salt grain sizes) the balance shifts in favor of power law flow. For a linear viscosity of 10^{19} Pa s there is a noticeable but small difference in maximum subsidence; this is 6% larger than with a linear flow law only. This is a consequence of more shear stress flow. Also, vertical velocities are faster initially. We therefore conclude that using a more accurate combined linear and power law flow law (instead of just a simpler linear one) will only have an effect on the subsidence evolution when the linear viscosity is relatively high, i.e., the grain size is large. For the *Carter et al.* [1993] mean parameters and the specific geomechanical model for the north of the Netherlands reservoir attempted, this happens only for 10^{19} Pa s. However, the situation is highly geometry dependent and as the shear stress magnitude is important, parameters like the distance of the rock salt layer to the reservoir or the magnitude of the reservoir pressure decrease and decrease rate would have an effect on this.

8.2. Use of a Power Law Creep Equation Only

For the simulations presented here we assume that the salt creep is described throughout the whole stress range by a single power law curve. Two flow laws from the literature have been attempted, one detailed in *ter Heege et al.* [2005a] and one often called the BGRa law [*Hunsche and Hampel*, 1999]. Note that neither of these laws is thought to be the best description of pure halite flow as required for this application, for different reasons. The ter Heege et al. creep law incorporates the effects of continuous grain size change that is thought to occur in rock salt at strains above 5–10%. A check on the resultant deviatoric strains after

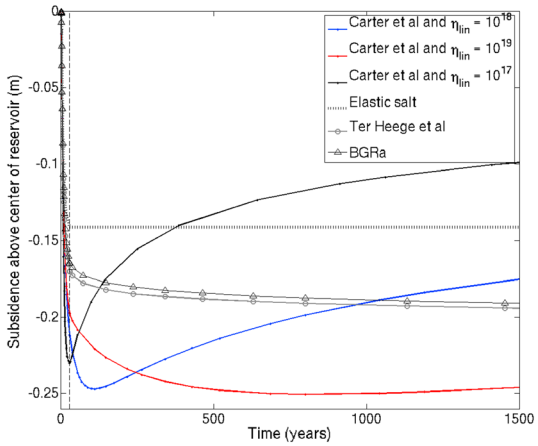

Figure 10. The evolution of maximum subsidence for the model where a realistic reservoir pore pressure history is applied. Results for a power law rock salt creep rheology only. The combined linear and Carter et al. power law flow results are included for reference. The vertical broken line represents end of pumping history, i.e., 28 years.

28 years of salt flow has shown that these are below 0.25% everywhere. This means that based on these strain levels alone, it is considered improbable that flow through that equation as dynamic salt recrystallization will not have developed. The BGRa flow law on the other hand is a fit to experimental data that were in part obtained under conditions where the rock salt might have lost water and are certainly for data obtained at higher stresses. It is, therefore, unclear whether it can be extrapolated to the low shear stress conditions relevant to our problem. Results of analyses that use these two flow laws will be shown nevertheless so as to illustrate the trends in the response to power law rock salt creep.

Figure 10 compares the maximum subsidence evolution for these two flow laws to the ones for the combined linear and *Carter et al.* [1993] law. For the same stress levels, the ter Heege and BGRa flow laws result in higher minimum viscosities (see Figure 11) and so lower strain rates (see Figure 2) than other flow laws if these are below approximately 1 MPa. They, therefore, lead to delayed subsidence increase. As can be seen in Figure 2a, of the two power law, only models at 100°C, the BGRa one produces lower strain rates for a given stress. As the problem is stress driven, i.e., in all simulations the shear stresses that initially develop inside the rock salt are primarily controlled by the pressure decrease in the reservoir, there is faster relaxation for the ter Heege et al. law and higher rate of change of maximum subsidence, leading to higher maximum subsidence values at the end of the forcing. A similar effect can be observed if A in equation (2) that describes rock salt flow is changed. For a given fixed value of n in the creep law, a larger A value leads to larger strain rates for a given stress, an accelerated subsidence increase, and a higher maximum subsidence value. This has been confirmed by simulations, the results of which are not shown here for brevity. In both power law models viscosities increase for low stresses, and the material creep rates become very low. This effectively "freezes" the situation at large times and blocks the development of the pressure flow mechanism. Subsidence rebound is therefore not observed (see Figure 10). As both flow laws result in comparable viscosities and strain rates at low stresses the decay behavior of the subsidence curve is similar at large times. This leads to only small differences in the maximum subsidence evolution at large times for these two creep laws.

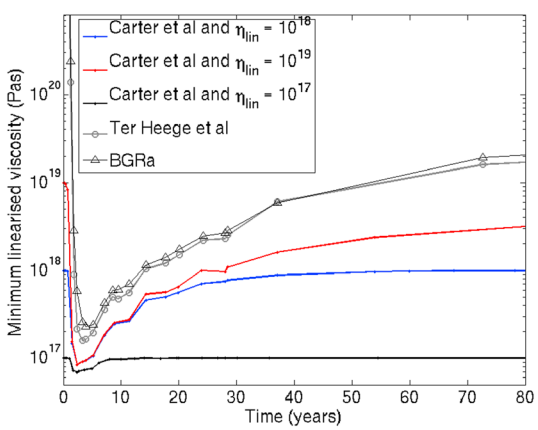

Figure 11. Evolution of the minimum linearized viscosity in the simulations that use the realistic pressure depletion history for a number of rock salt flow laws.

8.3. Implementation of a Stress Limit Below Which the Linear Creep Microprocess Gets Inhibited

The behavior at very low stresses is completely unknown as the strain rates are beyond what is experimentally measurable. Up to now we have assumed that microprocesses responsible for creep will continue indefinitely until the stresses relax completely. In this section we use a combined linear and Carter et al. power law creep law and impose an arbitrary stress limit below which pressure solution gets completely switched off. This means that below this stress the material reverts to the dislocation-controlled power law rates, which are many orders of magnitude smaller than ones due to pressure solution and decay very quickly as stress decreases. Note that this stress

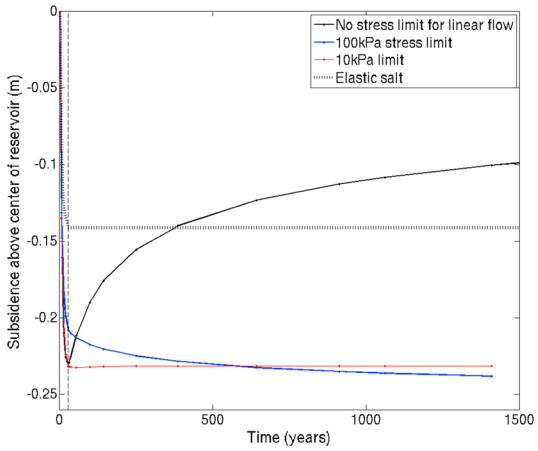

Figure 12. The evolution of maximum subsidence for the model where a realistic reservoir pore pressure history is applied. Results for a combined *Carter et al.* [1993] power law and a linear flow law with a viscosity of 10^{17} Pa s. The blue and red curves are for simulations where a stress limit of 100 kPa and 10 kPa has been applied, respectively, below which the linear flow law is deactivated and the rock salt flow reverts to the *Carter et al.* [1993] power law (which produces a much higher viscosity). The fully elastic rock salt layer results are included for reference. The vertical broken line represents end of pumping history, i.e., 28 years.

limit is not backed up by any experimental evidence and so the value of the stress limit is not constrained in any way. However a process that could lead to blockage of pressure solution is intergrain boundary healing [*van Noort et al.,* 2008]. This could inhibit ionic diffusion away from the stressed intergrain boundary by breaking up the fluid film pathway necessary for pressure solution (as discussed above). Figure 12 shows that even a very low stress limit (10 kPa) can lead to a complete change of behavior after the end of the gas production. Eventual subsidence rebound is not observed, confirming the link between linear creep and the pressure flow macroscale displacement mechanism. A 100 kPa limit switches off some of the stress relaxation too and so leads to a smaller subsidence increase than would have been calculated otherwise.

9. Approximating Transient Creep

All the above focuses on steady state creep even though transient creep may be relevant particularly to the initial stages of relaxation after the pore pressure reduction. This is because it is very common in modeling to focus on steady state creep [see, e.g., *Orlic and Wassing*, 2013; *Nikolinakou et al.,* 2014; *Breunese et al.,* 2003; *Luo et al.,* 2012, and references therein]. Transient creep is complex to model [see, e.g., *Carter et al.,* 1993]. The exact form of a transient creep constitutive law depends on both the initial conditions and also the path in the three-dimensional stress space followed by a particular material element. The simplest possible case for a stress increment is the application of a constant pure deviatoric stress to a sample already in static equilibrium. A schematic of the expected behavior is shown in Figure 13.

By lumping transient creep strains together with elastic strains, a relatively good approximation of the stress-strain curve can be obtained. This can be easily done by artificially reducing the elastic moduli of rock salt. Specifically, for rock salt, a Young's modulus that is a half to a quarter of the true elastic modulus of the material is sometimes used [e.g., *Prij*, 1991] along with a power law flow equation and/or linear viscous law, in order to approximate the transient creep behavior. This approach is not ideal and might produce artifacts, particularly as the bulk modulus of rock salt also gets reduced via the choice of Young's modulus. However, as we have noted, rock salt does not undergo much volume strain so that the effect of the reduction of the bulk modulus seems secondary.

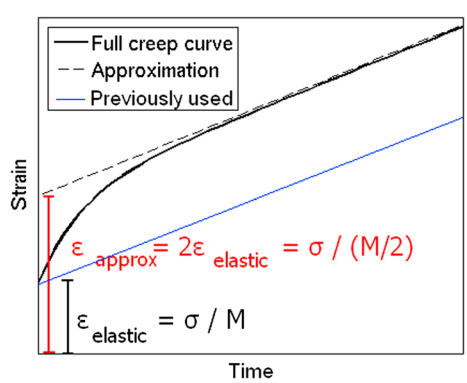

Figure 13. A sketch of the strain versus time plot for a material that displays transient creep, the curve used up to now in simulations (in blue), and an approximation to the transient curve that will be used in this section (dashed black line). *M* is the relevant elastic modulus (which is the shear modulus here).

Here we use a modified value of 15 GPa and 7.5 GPa for the salt Young's modulus (i.e., a half and a quarter of the original value), together with combined Carter et al. and linear (pressure solution) flow laws. Figure 14 shows that the rate of subsidence is initially slightly larger for the transient creep simulations. This might be attributed to the fact that the exact layering of the model has now changed, meaning that the apparent decay time of the first macroscale mechanism responsible

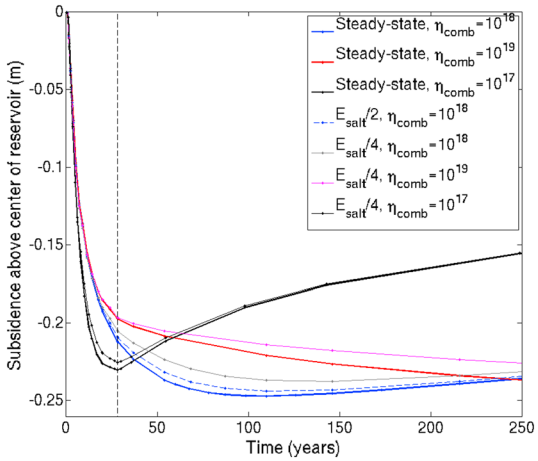

Figure 14. The evolution of maximum subsidence for the model where a realistic reservoir pore pressure history is applied. Results are shown for a combined linear and Carter et al. power law flow and include results for simulations in which the rock salt modulus has been reduced so as to approximate transient creep. The vertical broken line represents end of pumping history, i.e., 28 years.

for subsidence has changed slightly. On the other hand, the timescale for the second mechanism (pressure flow), responsible for the subsidence rebound, is primarily controlled by the rock salt Maxwell time for a constant rock salt layer thickness. As in the transient creep simulations, the rock salt element Maxwell time is larger than the original Maxwell time; the full subsidence rebound happens later. Maximum subsidence values are slightly affected and the overall conclusion might be that transient creep makes a small but measurable difference to the subsidence versus time curve. Care can be taken to model transient creep more accurately, but this only seems necessary if other uncertainties pertaining to the geomechanical model are resolved, as their effect on the subsidence calculation can be much larger.

It should be noted that this subsection also indirectly investigates the sensitivity to the rock salt elastic modulus, the exact value of which can vary slightly depending on salt composition. Note that for different salt layer compositions, *Breunese et al.* [2003] use a range of Young's modulus values between 5.5 and 30 GPa. Of course, an important consequence of the presence of salt of different composition is that creep constitutive model parameters will vary. Investigating the effects of salt composition on the overall behavior, notably on dislocation creep behavior [see *Wawersik and Zeuch*, 1986] though important, is beyond the scope of the current study.

10. Discussion, Implications for Modeling, and Conclusions

Work presented has investigated rock salt creep as a mechanism that can lead to time-dependent ground subsidence above a producing gas reservoir. Other possible causes of nonelastic, time-dependent subsidence have been completely neglected here but are possibly very important for some reservoirs at least (e.g., continuing reservoir creep or delayed poroelastic compaction of the surrounding material layers). This paper extends previous studies by *Marketos et al.* [2015a, 2015b] that were conducted on oversimplified geometries to a more realistic reservoir geomechanics model that, among others, includes the geological material layering and pressure depletion history. Importantly, the current paper also critically discusses different rock salt creep laws and assesses the implications of rock salt constitutive model choice on the subsidence evolution above a gas reservoir. It confirms that (for a specific representation of a producing north of the Netherlands gas field) salt flow can lead to time-dependent subsidence of up to 40% of what would have been calculated through elastic analyses only. The salt flow mechanism is therefore a very important contributor to the overall subsidence, and care should be taken to model rock salt creep as accurately as possible if accurate subsidence predictions are required. Note, however, that reservoir geometry (e.g., size) will be important in determining the amount of rock salt-induced time-dependent subsidence.

A major obstacle to achieving high accuracy of subsidence calculations is that there is no consensus in the literature as to which constitutive model best describes rock salt creep. Here we present available steady state creep laws for halite salt and focus the discussion on laws that come about either due to dislocation movement or pressure solution and ion migration across stress gradients. As both processes are assumed to be active at the same time within rock salt, the total strain rate can be calculated as the sum of the two individual strain rates. We note that there is evidence to suggest that pressure solution becomes rate controlling at relatively low stresses in the presence of small amounts of water within the halite rock. We further note that pressure solution leads to a linear flow law in which linear viscosity is grain size dependent, whereas dislocation-related flow laws lead to nonlinear flow laws that are to first order grain size independent.

Therefore, the stress range over which pressure solution is most important is larger for fine-grained rock salt, i.e., for the lower linear viscosity values. In these cases it is possible to just model the rock salt body with a linear creep law without much loss of accuracy in the subsidence calculation - see however section 8.3.

We discuss that if salt flow can be approximated as being by linear creep only then understanding the step response of the system, i.e., the response to a step decrease in reservoir pore pressure, becomes very important. This is because the response to any reservoir pore pressure decrease history can be calculated as the superposition of suitably-scaled step responses. Here we confirm the observation of *Marketos et al.* [2015a] that the step response can be separated out into two macroscale mechanisms by which displacement develops: Initially, a shear stress relaxation mechanism that leads to a deeper and narrower subsidence bowl is observed, followed by a pressure flow mechanism that leads to subsidence rebound and widening of the subsidence bowl. The timescales over which these two mechanisms develop are proportional to the timescale for relaxation of a rock salt material element, i.e., its Maxwell time, the ratio of the rock salt viscosity to the rock salt shear modulus.

We have also seen that the initial increase in the maximum subsidence at the surface in response to a step decrease of reservoir pressure can be described very well by an exponential decay, the decay time constant of which is much larger than the rock salt element decay time (Maxwell time). For the specific reservoir analyzed here this is approximately 13 times the rock salt Maxwell time. Hence, when calculating the subsidence response of a linear system to a reservoir pressure decrease applied over a fixed period, an important nondimensional quantity arises, the ratio of the timescale for pressure decrease in the reservoir to the timescale for the system's subsidence response. If this ratio is relatively small and the system responds rapidly to an applied pore pressure decrease (i.e., the rock salt has a sufficiently low viscosity), there is the potential that some pressure flow will occur before the end of gas production and pore pressure decrease. This means that there will already be some surface rebound before the end of production and that maximum subsidence values will be reduced when compared to higher rock salt viscosity situations.

Note, however, that linear viscosity of rock salt due to deformation by pressure solution creep is proportional to the third power of effective grain size [*Spiers et al.,* 1990]. Often, the grain size of a rock salt body is not known, as, typically, little core is recovered due to technical difficulties, leading to large uncertainties in the relevant viscosity value. For example, for the case of a salt body in the north of the Netherlands, *Breunese et al.* [2003] state that the effective mean grain size of rock salt is between 3 and 20 mm which leads to variations in linear (pressure solution) viscosity of over 2 orders of magnitude. This in turn gives rise to over 2 orders of magnitude uncertainty in the timescales over which time-dependent subsidence will develop. Other uncertainties are associated with the fact that it is typically difficult to determine how much water or impurities (e.g., other salts) a typical rock salt body contains. While the effects of water content variation on creep behavior are likely limited as only small amounts of water are necessary for the behavior to be "wet" [cf. *Ter Heege et al.,* 2005a, 2005b], large amounts of other salts or clays present as distributed or layered impurities may strongly affect the flow behavior of rock salt, thus affecting the time-dependent part of subsidence. Note, though, that better sampling of rock salt is not the solution; this can only be performed at point locations. So, even if rock salt core gets recovered successfully, the bulk of the rock salt behavior would still remain unknown as spatial heterogeneities in rock salt can be very large. In many cases, geological arguments as to the possible composition of salt at a specific location as affected by its deposition environment and subsequent deformation or diapirism [see, e.g., *Geluk*, 1998; *Geluk et al.,* 2007; *Urai et al.,* 2008], in conjunction with back-calculation of the material response from field situations where rock salt flow is important (e.g., *Breunese et al.* [2003] or *Li et al.* [2012]), can also be very informative. Note that geophysical exploration data can also help better understand the internal structure of salt bodies [see, e.g., *van Gent et al.,* 2011], as the presence of other evaporites can significantly affect the creep response of a salt body.

Analyses that have investigated the effect of other commonly used rock salt flow laws on the observed behavior have also been presented, so as to investigate the full extent of possible responses. As these flow laws are formulated on the basis of experiments at relatively high stresses, it is unclear whether data can be safely extrapolated to conditions relevant to a producing gas reservoir. In addition, some tests might have been conducted under conditions in which rock salt samples might have partially dried up, resulting in significantly higher viscosities when determined in the laboratory as compared to in situ rock salt. Finally, tests in which

the confining stress is low so that dilation cracks might have formed during creep would also have led to flow laws that are irrelevant to the reservoir geomechanics application discussed.

This said, available power law-only creep equations lead to no observation of subsidence rebound, i.e., no development of the pressure flow macroscale mechanism at large times after the end of gas production. This is because this mechanism is only active at low shear stresses within the rock salt, and power law rheologies lead effectively to "freezing" (large increase of viscosity) of the material at low stresses. The pressure flow mechanism is also not observed in analyses where we have somewhat arbitrarily inhibited linear flow (i.e., have assumed that the pressure solution microprocess gets blocked), further confirming the link between subsidence rebound and the relatively low viscosity behavior of in situ rock salt at low stresses. As the low stress behavior of rock salt is impossible to determine experimentally, the only piece of information that could give some evidence as to it is again field data from subsidence over abandoned gas reservoirs or salt mines (e.g., the salt mine at Barradeel in studies similar to *Breunese et al.* [2003] or *van Heekeren et al.* [2009]) provided that the salt physical properties are similar to the rock salt above a gas reservoir. The authors are not aware of any field data for abandoned hydrocarbon reservoirs that have exhibited this subsidence rebound. This could be due to the lack of data; only time can confirm whether a linear creep constitutive model is also applicable to rock salt flow at very low shear stresses.

This study has focused on investigating the effect of steady state creep of rock salt on subsidence above a producing gas field. Transient creep is also important if determining the exact time dependence of surface subsidence is necessary, especially during the gas production period. However, our inclusion of an approximation of transient creep effects has indicated that differences between model results that incorporate it and ones that do not are not very large. These would be dwarfed by differences in results due to uncertainties in the grain size-dependent creep properties of rock salt and other geomechanical model uncertainties such as the composition of rock salt.

The main conclusion from this study is that for a medium-sized rock salt-capped reservoir one would expect significant time-dependent displacements due to rock salt flow. This is irrespective of the constitutive model used to describe rock salt creep. This time-dependent subsidence would be in addition to the one due to other mechanisms such as reservoir rock creep or delayed poroelastic compaction due to pore pressure equilibration. Neglecting rock salt-induced time-dependent subsidence has the consequence of underestimating surface subsidence magnitudes and so should be avoided. Our results show, however, that the timescales over which this subsidence develops cannot be practically constrained due to the large uncertainties in the rock salt creep constitutive model which are in turn linked to large uncertainties in rock salt grain size, water content, and composition spatial variation. In response to these uncertainties the only possible solution for geomodelers seems to be the calculation of bounds on the predicted future subsidence levels through the use of end-member scenaria for the rock salt creep flow laws. The identification of possible rock salt flow laws that are relevant to a specific site (as affected by rock salt physical properties) can be performed on the basis of the thorough discussion of rock salt flow laws presented here.

Acknowledgments
This work is a partial output of a project funded by NAM BV, the Dutch gas fields operator, as part of an independent study set up to investigate subsidence effects in the Waddenzee area in the north of the Netherlands. Discussions with Tony Mossop (Shell) and Rob van Eijs (NAM), and the comments of Yves Bernabe (MIT) and an anonymous reviewer are gratefully acknowledged. The data for this paper are available by contacting the corresponding author at g.marketos.99@cantab.net.

References

Baes, M., R. Govers, and R. Wortel (2011), Switching between alternative responses of the lithosphere to continental collision, *Geophys. J. Int.*, *187*, 1151–1174.

Balay, S., K. Buschelman, W. D. Gropp, D. Kaushik, M. Knepley, L. Curfman McInnes, B. F. Smith, and H. Zhang (2002), PETSc users manual, Argonne Natl. Lab.

Bérest, P., J. F. Béraud, M. Bourcier, A. Dimanov, H. Gharbi, B. Brouard, K. DeVries, and D. Tribout (2012), Very slow creep tests on rock samples, in *Proceedings of the Mechanical Behavior of Salt VII*, edited by P. Bérest et al., pp. 81–88, Taylor and Francis, London.

Blanco Martín, L., L. Rutqvist, and J. T. Birkholzer (2015), Long-term modeling of the thermal-hydraulic-mechanical response of a generic salt repository for heat-generating nuclear waste, *Eng. Geol.*, *193*, 198–211.

Bolton, M. D. (1991), *A Guide to Soil Mechanics*, 2nd ed., MD & K Bolton Publishers, Cambridge, U. K.

Breunese, J. N., R. M. H. E. van Eijs, S. de Meer, and I. C. Kroon (2003), Observation and prediction of the relation between salt creep and land subsidence in solution mining—The Barradeel case, paperpresented at SMRI Conference, Chester.

Buiter, S. J. H., R. Govers, and M. J. R. Wortel (2001), A modelling study of vertical surface displacements at convergent plate margins, *Geophys. J. Int.*, *147*, 415–427.

Carter, N. L., S. T. Horseman, J. E. Russel, and J. Handin (1993), Rheology of rocksalt, *J. Struct. Geol.*, *15*, 1257–1271.

Coelewij, P. A. J., G. M. W. Haug, and H. van Kuijk (1978), Magnesium-salt exploration in the Northeastern Netherlands, *Geol. Mijnbouw*, *57*, 487–502.

De Franco, R., R. Govers, and R. Wortel (2007), Numerical comparison of different convergent plate contacts: Subduction channel and subduction fault, *Geophys. J. Int.*, *171*, 435–450.

Desbois, G., P. Závada, Z. Schléder, and J. L. Urai (2010), Deformation and recrystallization mechanisms in actively extruding salt fountain: Microstructural evidence for a switch in deformation mechanisms with increased availability of meteoric water and decreased grain size (Qum Kuh, central Iran), *J. Struct. Geol.*, *32*, 580–594.

Dribus, J. R., M. P. A. Jackson, J. Kapoor, and M. F. Smith (2008), The prize beneath the salt, *Oilfield Rev.*, *20*, 4–17.

Frost, H. J., and M. F. Ashby (1982), *Deformation-Mechanism Maps: The Plasticity and Creep of Metals and Ceramics*, Pergamon Press, Oxford, U. K.

Furlong, K. P., and R. Govers (1999), Ephemeral crustal thickening at a triple junction: The Mendocino crustal conveyor, *Geology*, *27*, 127–130.

Gambolati, G., P. Teatini, and M. Ferronato (2006), Anthropogenic land subsidence, *Encycl. Hydrol. Sci.*, *13*, 158.

Geluk, M. C. (1998), Internal tectonics of salt structures, *J. Seismic Explor.*, *7*, 237–251.

Geluk, M. C., W. A. Paar, and P. A. Fokker (2007), Salt, in *Geology of the Netherlands*, edited by T. E. Wong, D. A. J. Batjes, and J. De Jager, pp. 283–294, R. Netherlands Acad. of Arts and Sci., Amsterdam.

Gerya, T. V. (2010), *Introduction to Numerical Geodynamic Modelling*, pp. 260–261, Cambridge Univ. Press, Cambridge, U. K.

Govers, R., and M. J. R. Wortel (1993), Initiation of asymmetric extension in continental lithosphere, *Tectonophysics*, *223*, 75–96.

Govers, R., and M. J. R. Wortel (1995), Extension of stable continental lithosphere and the initiation of lithosphere scale faults, *Tectonics*, *14*, 1041–1055, doi:10.1029/95TC00500.

Govers, R., and M. J. R. Wortel (1999), Some remarks on the relation between vertical motions of the lithosphere during extension and the "necking depth" parameter inferred from kinematic modeling studies, *J. Geophys. Res.*, *104*, 23,245–23,254, doi:10.1029/1999JB900201.

Govers, R., and M. J. R. Wortel (2005), Lithosphere tearing the STEP faults: Response to edges of subduction zones, *Earth Planet. Sci. Lett.*, *236*, 505–523.

Günther, R.-M., K. Salzer, T. Popp, and C. Lüdeling (2015), Steady-state creep of rock salt: Improved approaches for lab determination and modelling, *Rock Mech. Rock Eng.*, 1–11.

Hall-Wallace, M., and H. J. Melosh (1994), Buckling of a pervasively faulted lithosphere, *Pure Appl. Geophys.*, *142*, 239–261.

Hettema, M., E. Papamichos, and P. Schutjens (2002), Subsidence delay: Field observations and analysis, *Oil Gas Sci. Technol. – Rev. IFP*, *57*, 443–458.

Horii, H. L., and S. Nemat-Nasser (1985), Compression-induced microcrack growth in brittle solids: Axial splitting and shear failure, *J. Geophys. Res.*, *90*, 3105–3125, doi:10.1029/JB090iB04p03105.

Hunsche, U., and A. Hampel (1999), Rock salt—The mechanical properties of the host rock material for a radioactive waste repository, *Eng. Geol.*, *52*, 271–291.

Ketelaar, V. B. H. (2009), *Satellite Radar Interferometry: Subsidence Monitoring Techniques*, Springer. [Available at https://books.google.gr/books?id=pT3ug1Ij4cQC&printsec=frontcover&dq=Satellite+Radar+Interferometry:+Subsidence+Monitoring+Techniques&hl=el&sa=X&ved=0ahUKEwiJvezpzbTNAhUqD8AKHag2AwoQ6AEIHjAA#v=onepage&q=Satellite%20Radar%20Interferometry%3A%20Subsidence%20Monitoring%20Techniques&f=false.]

Li, S., S. Abe, J. L. Urai, F. Strozyk, P. A. Kukla, and H. van Gent (2012), A method to evaluate long-term rheology of Zechstein salt in the Tertiary, in *Mechanical Behaviour of Salt VII*, edited by P. Bérest et al., pp. 215–220, Taylor and Francis, London.

Luo, G., M. A. Nikolinakou, P. B. Flemings, and M. R. Hudec (2012), Geomechanical modeling of stresses adjacent to salt bodies: Part 1—Uncoupled models, *Am. Assoc. Pet. Geol. Bull.*, *96*, 43–64.

Lux, K. H., and S. Heusermann (1983), Creep tests on rock salt with changing load as a basis for the verification of theoretical material laws, in *Proceedings of 6th Symposium on Salt, Toronto*, vol. I, pp. 417–435, Salt Inst., Alexandria, Va.

Marketos, G., R. Govers, and C. J. Spiers (2015a), Ground motions induced by a producing hydrocarbon reservoir that is overlain by a viscoelastic rocksalt layer: A numerical model, *Geophys. J. Int.*, *203*, 228–242.

Marketos, G., R. Govers, and C. J. Spiers (2015b), Surface subsidence induced by hydrocarbons extraction, and the potential for time-dependent ground deformations, in *Proceedings of the 49th US Rock Mechanics/ Geomechanics Symposium*, 7 pp., Am. Rock Mech. Assoc., San Francisco, Calif.

Mohriak, W. U., P. Szatmari, and S. Anjos (2012), Salt: Geology and tectonics of selected Brazilian basins in their global context, *Geol. Soc. London Spec. Publ.*, *363*, 131–158.

Mossop, A. (2012), An explanation for anomalous time dependent subsidence, in *Proceedings of the 46th US Rock Mechanics/Geomechanics Symposium*, 8 pp., Am. Rock Mech. Assoc., Chicago.

Muhammad, N., C. J. Spiers, C. J. Peach, and J. H. P. de Bresser (2012), Effect of confining pressure on plastic flow of salt at 125°C, in *Mechanical Behaviour of Salt VII*, edited by P. Bérest et al., pp. 57–64, CRC Press, London.

Munson, D. E., and P. R. Dawson (1979), Constitutive Model for the Low Temperature Creep of Salt (With Application to WIPP) SAND79-1853, Sandia Natl. Lab., Albuquerque, N. M.

Munson, D. E., A. F. Fossum, and P. E. Senseny (1990), Approach to first principles model prediction of measured WIPP (Waste Isolation Pilot Plant) in-situ room closure in salt, *Tunnelling Underground Space Technol.*, *5*, 135–139.

Nagel, N. B. (2001), Compaction and subsidence issues within the petroleum industry: From Wilmington to Ekofisk and beyond, *Phys. Chem. Earth A*, *26*, 3–14.

Nederlandse Aardolie Maatschappij (NAM) (2010), Bodemdaling door Aardgaswinning: Statusrapport 2010 en Prognose tot het jaar 2070. [Available at http://www.commissiebodemdaling.nl/files/nam_bodemdalingsrapport2010.pdf, Accessed June 4th, 2015].

Nederlandse Aardolie Maatschappij (NAM) (2013), Technical addendum to the Winningsplan Groningen 2013: Subsidence, induced earthquakes and seismic hazard analysis in the Groningen Field. [Available at http://www.rijksoverheid.nl/bestanden/documenten-en-publicaties/rapporten/2014/01/17/bijlage-1-analyse-over-verzakkingen-geinduceerde-aardbevingen-en-seismische-risico-s/2-2-a-technical-addendum-to-the-winningsplan-groningen-2013.pdf].

Nikolinakou, M. A., P. B. Flemings, and M. R. Hudec (2014), Modeling stress evolution around a rising salt diapir, *Mar. Pet. Geol.*, *51*, 230–238.

Orlic, B., and B. B. T. Wassing (2013), A study of stress change and fault slip in producing gas reservoirs overlain by elastic and viscoelastic caprocks, *Rock Mech. Rock Eng.*, *46*, 421–435.

Peach, C. J., C. J. Spiers, and P. W. Trimby (2001), Effect of confining pressure on dilatation, recrystallization, and flow of rock salt at 150°C, *J. Geophys. Res.*, *106*, 13,315–13,328, doi:10.1029/2000JB900300.

Plattner, C., F. Amelung, S. Baker, R. Govers, and M. Poland (2013), The role of viscous magma mush spreading in volcanic flank motion at Kīlauea Volcano, Hawai'i, *J. Geophys. Res. Solid Earth*, *118*, 2474–2487, doi:10.1002/jgrb.50194.

Prij, J. (1991), On the design of a radioactive waste repository, PhD thesis, Univ. of Twente, p. 227.

Raith, A. F., F. Strozyk, J. Visser, and J. L. Urai (2015), Evolution of rheologically heterogeneous salt structures: A case study from the northeast of the Netherlands, *Solid Earth Discuss.*, *7*, 1877–1908.

Riva, R. E. M., and R. Govers (2009), Relating viscosities from postseismic relaxation to a realistic viscosity structure for the lithosphere, *Geophys. J. Int.*, *176*, 614–624.

Schléder, Z., and J. L. Urai (2007), Deformation and recrystallization mechanisms in mylonitic shear zones in naturally deformed extrusive Eocene–Oligocene rocksalt from Eyvanekey plateau and Garmsar hills (central Iran), *J. Struct. Geol.*, *29*, 241–255.

Schléder, Z., S. Burlinga, and J. L. Urai (2007), Dynamic and static recrystallization-related microstructures in halite samples from the Kłodawa salt wall (central Poland) as revealed by gamma-irradiation, *Neues Jahrb. Mineral.-Abh.: J. Mineral. Geochem.*, *184*, 17–28.

Schmalzle, G., T. Dixon, R. Malservisi, and R. Govers (2006), Strain accumulation across the Carrizo segment of the San Andreas Fault, California: Impact of laterally varying crustal properties, *J. Geophys. Res.*, *111*, B05403, doi:10.1029/2005JB003843.

Spiers, C. J., and N. L. Carter (1998), Microphysics of rocksalt flow in nature, in *The Mechanical Behavior of Salt, Proceedings of the 4th Conference, Trans Tech. Publ. Ser. on Rock and Soil Mech.*, vol. 22, edited by M. Aubertin and H. R. Hardy, pp. 115–128, Trans. Tech. Publ., Clausthal.

Spiers, C. J., P. M. T. M. Schutjens, R. H. Brzesowsky, C. J. Peach, J. L. Liezenberg, and H. J. Zwart (1990), Experimental determination of constitutive parameters governing creep of rocksalt by pressure solution, in *Deformation Mechanisms, Rheology and Tectonics*, edited by R. J. Knipe and E. H. Rutter, *Geol. Soc. London Spec. Publ.*, 54, 215–227.

Ter Heege, J. H., J. H. P. De Bresser, and C. J. Spiers (2005a), Rheological behaviour of synthetic rocksalt: The interplay between water, dynamic recrystallization and deformation mechanisms, *J. Struct. Geol.*, *27*, 948–963.

Ter Heege, J. H., J. H. P. De Bresser, and C. J. Spiers (2005b), Dynamic recrystallization of wet synthetic polycrystalline halite: Dependence of grain size distribution on flow stress, temperature and strain, *Tectonophysics*, *396*, 35–57.

Urai, J. L., and C. J. Spiers (2007), The effect of grain boundary water on deformation mechanisms and rheology of rocksalt during long-term deformation, in *Proceedings of the 6th Conference on the Mechanical Behavior of Salt—Understanding of THMC Processes in Salt*, edited by M. Wallner et al., pp. 149–158, Taylor and Francis, London.

Urai, J. L., C. J. Spiers, H. J. Zwart, and G. S. Lister (1986), Weakening of rock salt by water during long-term creep, *Nature*, *324*, 554–557.

Urai, J. L., C. J. Spiers, C. J. Peach, R. Franssen, and J. L. Liezenberg (1987), Deformation mechanisms operating in naturally deformed halite rocks as deduced from microstructural investigations, *Geol. Mijnbouw*, *66*, 165–176.

Urai, J. L., Z. Schléder, C. J. Spiers, and P. A. Kukla (2008), Flow and transport properties of salt rocks, in *Dynamics of Complex Intracontinental Basins: The Central European Basin System*, edited by R. Littke et al., pp. 277–290, Springer, Berlin.

Van Gent, H., J. L. Urai, and M. de Keijzer (2011), The internal geometry of salt structures—A first look using 3D seismic data from the Zechstein of the Netherlands, *J. Struct. Geol.*, *33*, 292–311.

Van Heekeren, H., T. Bakker, T. Duquesnoy, and V. de Ruiter (2009), Abandonment of an extremely deep Cavern at Frisia Salt, in *Proceedings of SMRI Spring 2009 Technical Conference*, SMRI, Clarks Summit, Pa.

Van Noort, R., H. J. M. Visser, and C. J. Spiers (2008), Influence of grain boundary structure on dissolution controlled pressure solution and retarding effects of grain boundary healing, *J. Geophys. Res.*, *113*, B03201, doi:10.1029/2007JB005223.

Van Thienen-Visser, K., J. N. Breunese, and A. G. Muntendam-Bos (2015), Subsidence due to gas production in the Wadden Sea: How to ensure no harm will be done to nature, in *Proceedings of the 49th US Rock Mechanics/Geomechanics Symposium*, ARMA, San Francisco.

Vasco, D. W., A. Ferretti, and F. Novali (2008), Reservoir monitoring and characterization using satellite geodetic data: Interferometric synthetic aperture radar observations from the Krechba field, Algeria, *Geophysics*, *73*, WA113–WA122.

Verruijt, A. (1996), Complex variable solutions of elastic tunnelling problems, Geotech. Lab., Delft Univ. of Technol. [Available at http://geo.verruijt.net/software/Tunnels.zip].

Wawersik, W. R., and D. H. Zeuch (1986), Modeling and mechanistic interpretation of creep of rock salt below 200°C, *Tectonophysics*, *121*, 125–152.

Wolters, R., K.-H. Lux, and U. Düsterloh (2012), Evaluation of rock salt barriers with respect to tightness: Influence of thermomechanical damage, fluid infiltration and sealing/healing, in *Proceedings of the 7th International Conference on Mechanical Behavoir of Salt (SaltMech7), Paris, France*, edited by P. Bérest et al., pp. 417–426, Taylor and Francis, London.

Yu, Y., L. Tang, W. Yang, T. Huang, N. Qiu, and W. Li (2014), Salt structures and hydrocarbon accumulations in the Tarim Basin, northwest China, *AAPG Bull.*, *98*, 135–159.